IMPROVEMENT IN ELECTROCHEMICAL PERFORMANCES OF Mm(NiCoMnAl)$_5$ ELECTRODES BY SURFACE MODIFICATION①

Chen Weixiang
Department of Materials Science and Engineering, Zhejiang University, Hangzhou 310027, P. R. China

ABSTRACT All metal elements on the surface of the hydrogen storage alloys exist in oxide state. The oxide layer on the surface of alloys affects the electrochemical performances of metal hydride (MH) electrodes. The surface of MH electrode was modified by immersing in 0.05 mol/L KBH_4+ 6 mol/L KOH or 0.2 mol/L NaH_2PO_2+ 6 mol/L KOH solution. It is found that their electrochemical properties such as discharge capacity, activation and cyclic stability are apparently improved. The effects of the mentioned surface modifications on the activity of electrochemical reaction were investigated by means of cyclic voltammetry (CV) and electrochemical impedance spectra (EIS). It is found that the surface modifications considerably improve the electrochemical activity and decrease the activation enthalpy of electrode reaction.

Key words metal hydride electrodes surface modification electrochemical performances CV EIS

1 INTRODUCTION

Nickel-metal hydride (Ni/MH) batteries have higher energy and capacity density, higher charge-discharge rate capability and environmental advantage compared with Ni-Cd batteries[1, 2]. Many multicomponent mischmetal-based hydrogen storage alloys have been employed for commercialized cells[2-4]. The surface properties of the alloys are very important for their electrochemical application. The electrochemical performances of the MH electrodes are influenced by the bulk composition as well as their surface composition, elemental chemical state and morphology. Various surface modifications[5-8] and additives dopes[9, 10] to alloy particle and MH electrodes have been proposed in order to improve their activation property, charge-discharge performance, high-rate dischargeability and cycle life.

In the present paper, the effects of surface modification of MH electrodes using KBH_4 or NaH_2PO_2 as reductant in alkaline solution on their activation, capacity, cyclic stability were investigated. The cyclic voltammetry (CV) and electrochemical impedance spectra (EIS) were employed to evaluate the effects of surface modifications on the electrochemical activity of MH electrodes.

2 EXPERIMENTAL

2.1 Preparation and surface modifications of MH electrodes

The hydrogen storage alloy Mm(NiCoMnAl)$_5$ (Mm= Ce-rich mischmetal: La 28.3%, Ce50.5%, Pr5.4%, Nd15.9%, other rare earth 0.3%) powder (44~74 μm, about 0.7 g) and 10% nickel powder were mixed well with a small amount of 2% polyvinylalcohol (PVA) solution, the mixture was scrubbed onto a porous foamed nickel substrates (2 cm^2) and then dried

① Project 863-715-004-0060 supported by the National Advanced Materials Committee of China
Received Jul. 9, 1997; accepted Nov. 18, 1997

in vacuum and finally pressed at a pressure of 500 MPa to form a test electrode. The MH electrodes were modified by immersing in 6 mol/L KOH+ 0.05 mol/L KBH_4 solution or 6 mol/L KOH+ 0.2 mol/L NaH_2PO_2 at 70 ℃ for 8 h.

2.2 Measurements of crystallographic and thermodynamic properties of alloy and electrochemical performances of MH electrode

Crystal structure and lattice parameters of the hydrogen storage alloy were determined by powder X-ray diffraction (XRD) using D/MAX-IIIA X-ray diffractometer with CuK_α radiation and a graphite diffracted-beam filter. Pressure composition isothermals (p —c —T) of the activated alloy were measured by an electrochemical method[11]. Both enthalpy change ΔH and entropy change ΔS of hydride formation were calculated by Van't Hoff equation:

$$\ln p_{eq} = \frac{\Delta H}{RT} - \frac{\Delta S}{R} \quad (1)$$

Electrochemical measurements were carried out using a three compartments glass cell separated with a sintered glass. The MH electrode was positioned in the central compartment and two counter nickel hydroxide electrodes with a larger electrochemical capacity were placed in compartments on each side. The reference electrode was a Hg/HgO (6 mol/L KOH) electrode. The electrolyte was a deaerated 6 mol/L KOH+ 20 g/L LiOH solution. Galvanostatic charge-discharge cycling test was performed at room temperature. MH electrode was charged for 3.5 h and discharged to − 0.6 V vs Hg/HgO with a pause of 10 min, both at a constant current density of 100 mA/g. In measuring the high-rate dischargeability, the MH electrode was charged at 100 mA/g for 3.5 h first, paused for 10 min, and then discharged at various current densities (250~ 1500 mA/g). The high-rate discharge ability was determined by the ratio (C/C_{100}), the discharge capacities measured at different current densities to that at 100 mA/g.

Cyclic voltammetries for the unmodified and modified MH electrodes were carried out in the potential region− 0.3~ − 1.3 V vs Hg/HgO at a sweep rate of 40 mV/s using an electrochemical testing system. The EIS measurements were carried out at about 50% DOD (depth of discharge) under open-circuit conditions by using a Solartron 1250 frequency response analyser and a Solartron 1286 potentiastat. EIS of the electrodes were recorded from 10000 Hz to 0.002 Hz by 5 mV perturbation. The EIS were analysed with the non-linear least squares fitting (NLLSF) program EQUIVCRT. Charge-transfer resistance R_{ct}, which is related to electrochemical activity of the alloy surface, was also determined. The activation enthaply $\Delta_r H$ of the MH electrode reaction was calculated from R_{ct} at different temperatures using the following equation[12]:

$$\ln\left(\frac{T}{R_{ct}}\right) = C_0 - \frac{\Delta_r H}{RT} \quad (2)$$

where C_0 is a constant in which the surface area of the MH electrode is included.

3 RESULTS AND DISCUSSION

3.1 Crystal structure and thermodynamic properties of hydrogen storage alloy

An XRD pattern for the alloy is shown in Fig. 1. The alloy crystal is a single phase of hexagonal $CaCu_5$-type structure. Lattice parameters (a and c) and unit cell volume (V) of the alloy are calculated to be a= 0.496 11 nm, c= 0.403 28 nm and V= 0.085 96 nm^3 by the following equations:

$$\frac{1}{d^2} = \frac{3}{4}\cdot\frac{h^2+h\cdot k+k^2}{a^2} + \frac{l^2}{c^2} \quad (3)$$

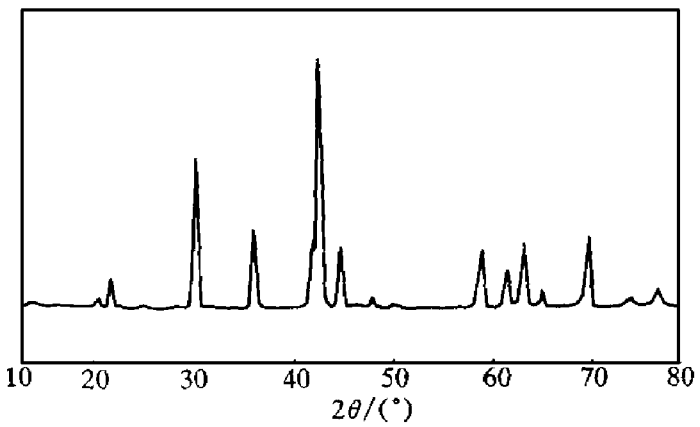

Fig. 1 XRD pattern for hydrogen storage alloy

$$V = \frac{\sqrt{3}}{2} \cdot a^2 \cdot c^2 \quad (4)$$

The p —c —T curves for the alloy at different temperatures and its Van' t Hoff plots are illustrated in Fig. 2 and Fig. 3 respectively. The enthalpy change ΔH and entropy change ΔS of hydride formation were evaluated to be − 33.76 KJ·mol^{-1} and − 101.52 J·mol^{-1}·K^{-1} respectively.

3.2 Activation property, discharge capacity and cyclic stability for MH electrodes

The activation profile and discharge capacities of the unmodified and KBH_4- and NaH_2PO_2-modified electrodes as a function of cycle number are shown in Fig. 4 and Fig. 5 respectively. The unmodified MH electrode shows a smaller initial capacity (< 100 mAh/g) as there is an oxide layer on the surface of the alloy. However, KBH_4- and NaH_2PO_2-modified electrodes show better activation properties and have larger initial discharge capacities. The maximum capacities of unmodified, KBH_4- and NaH_2PO_2-modified electrodes are up to 220, 275 and 255 mAh/g, respectively, in the experiment. At the 400th cycle, their capacities were 154, 248 and 221 mAh/g, respectively, cut down by 30.0%, 8.46% and 13.3% of their maximum capacities. These facts indicate that the surface modifications improve the activation property, cyclic stability and discharge capacity of MH electrodes.

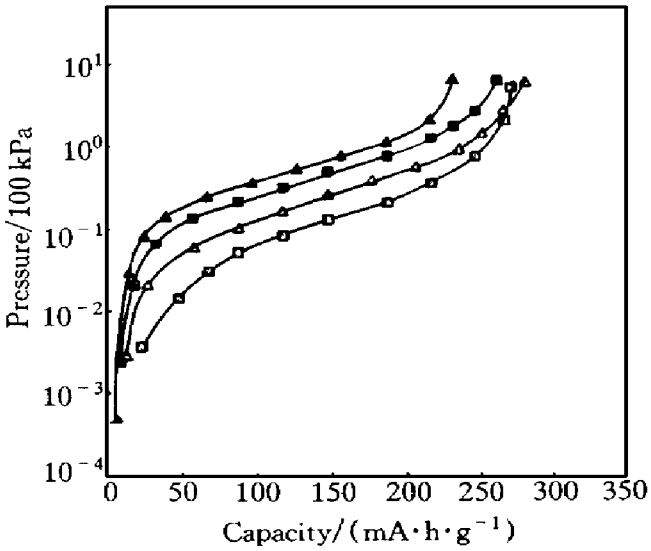

Fig. 2 p —c —T curves for hydrogen storage alloy

□ —10 ℃; △ —25 ℃; ■ —40 ℃; ▲ —50 ℃

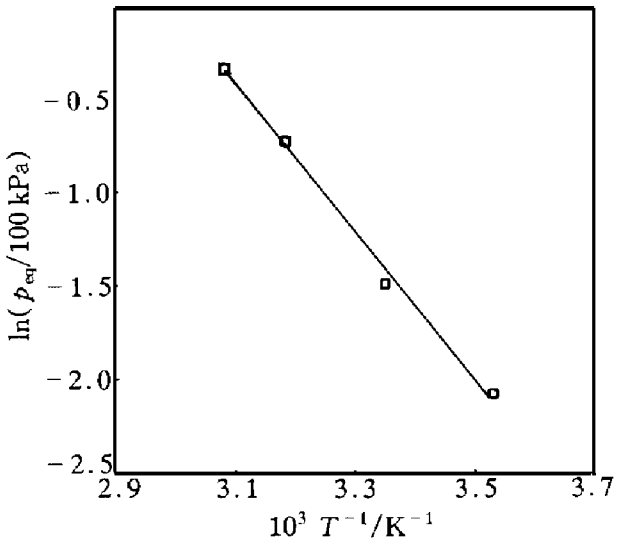

Fig. 3 Van' t Hoff plots for hydrogen storage alloy

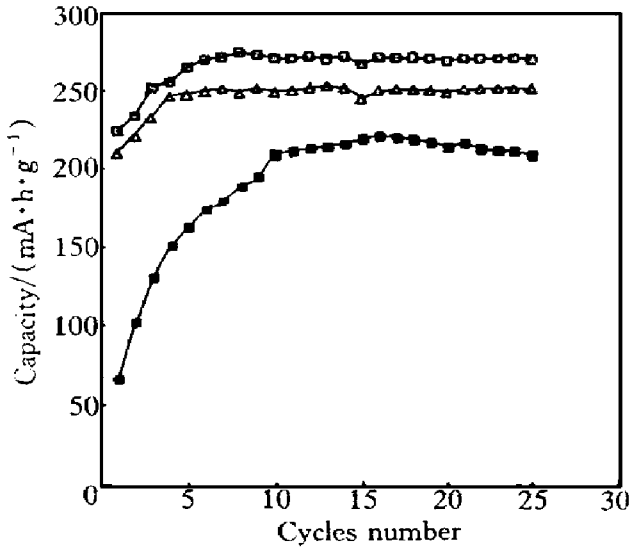

Fig. 4 Activation profile of MH electrodes

■ —Unmodified electrode;

□ —KBH_4-modified electrode;

△ —NaH_2PO_2-modified electrode

The high-rate dischargeabilities of the electrodes were measured after 15 cycle charge-discharge activation. As shown in Fig. 6, the surface modifications considerably improve the high-rate dischargeabilities of MH electrodes. In principle, the high-rate discharge ability is determined by the electrochemical activity on the electrode surface and the diffusion rate of hydrogen in the lattice of alloy. The results of XPS

and ICP analyses indicate[13] that the oxide film on the alloy surface would be reduced or eliminated by the surface modification because of the dissolution and reduction of oxide. A Ni-rich surface layer with high electrochemical activity is produced by preferential dissolution of Mn and Al. In addition, the surface modifications increase the specific surface area of the MH electrodes. Thus, the surface modifications raise the electrochemical activity of MH electrode and improve the high-rate discharge ability.

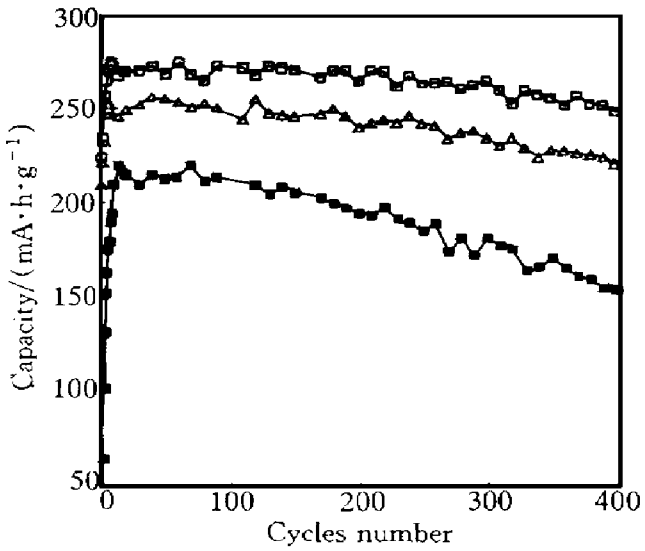

Fig. 5 Discharge capacities of MH electrodes as a function of cycle number

■ —Unmodified electrode;
□ —KBH_4-modified electrode;
△ —NaH_2PO_2-modified electrode

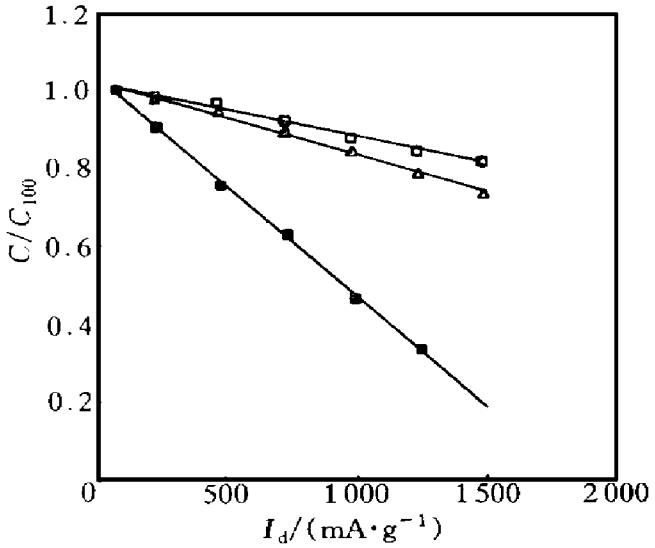

Fig. 6 High-rate dischargeability of MH electrodes

■ —Unmodified electrode;
□ —KBH_4-modified electrode;
△ —NaH_2PO_2-modified electrode

3.3 Cyclic voltammetry of MH electrodes

Before CV measurement, cyclic sweep was carried out for 10 cycles in the range − 0.3 V ~ − 1.3 V vs Hg/HgO at a sweep rate of 40 mV/s in order to make the unmodified MH electrode have a certain high electrochemical activity and hydrogen amount in the alloy. The cyclic voltammograms for unmodified, KBH_4- and NaH_2PO_2-modified electrodes are shown in Fig. 7. In anodic branch, anodic peaks are observed at around − 0.62 ~ − 0.65 V vs Hg/HgO for three electrodes, which is attributed to the oxidation of absorbed hydrogen. However, the peak is higher for KBH_4- or NaH_2PO_2-modified MH electrode than untreated one because the modified electrodes have larger initial capacities. The anodic peak of unmodified electrode is so broad that oxidation reaction of absorbed hydrogen is estimated to proceed rather slowly[14]. Therefore, it is understandable that the discharge step on the electrode surface controls the overall oxidation reaction of hydrogen because of a low electrochemical activity for the unmodified electrode. KBH_4- and NaH_2PO_2-modified MH electrodes show sharp anodic peaks, which means the oxidation reaction of hydrogen on the MH electrode surface proceeds smoothly. The facts indicate that the surface modifications improve electrochemical activity of oxidation reaction of hydrogen on MH electrode surface.

In cathodic branch of CV, there is a plateau attributed to adsorption of the atomic hydrogen on MH electrode surface. However, the plateau of KBH_4- or NaH_2PO_2-modified MH electrode is more obvious and much higher than that of unmodified MH electrode because of the enhancement of adsorption of the atomic hydrogen caused by their Ni-rich surface layer and increase in specific surface area.

3.4 EIS for MH electrodes

The typical EIS of MH electrode is shown in Fig. 8. The cole-cole plots consist of two obvious comparable semicircles and one slope. The

semicircle in high-frequency region is attributed to the contact resistance between the alloy particle and the current collector, the semicircle in low-frequency region is attributed to an electrochemical reaction on the electrode surface, and the slope is caused by the diffusion of hydrogen in the alloy. The equivalent circuit for EIS of MH electrode is expressed in Fig. 9. The parameters are evaluated by the non-linear least-squares fitting programme EQUIVCRT within the measured frequency region. The results are listed in Table 1.

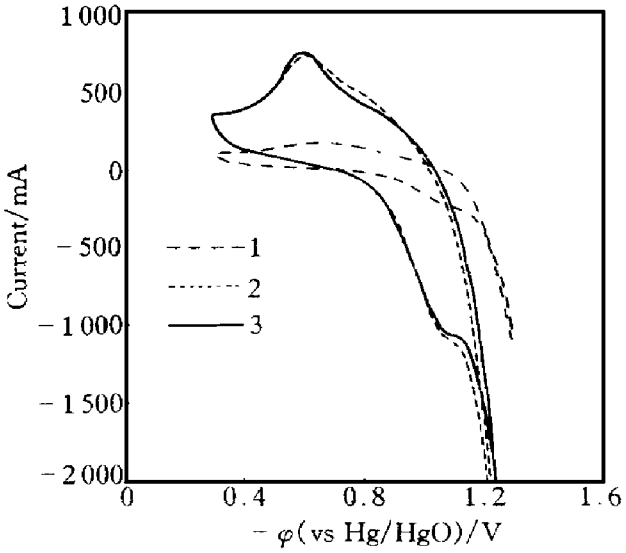

Fig. 7 Cyclic voltammograms of MH electrodes

1 —Unmodified electrode;
2 —NaH_2PO_2-modified electrode;
3 —KBH_4-modified electrode

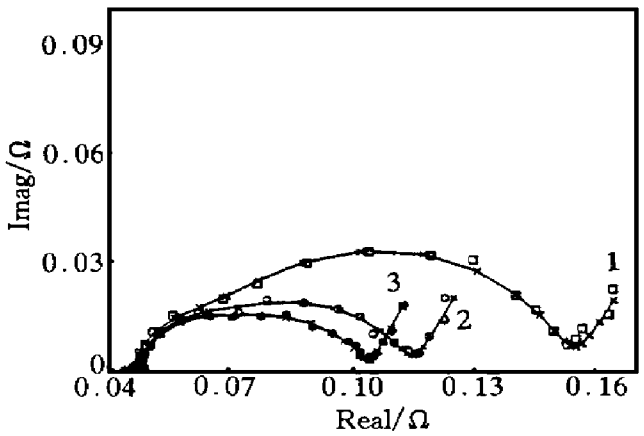

Fig. 8 EIS for MH electrodes

1 —Unmodified electrode;
2 —NaH_2PO_2-modified electrode;
3 —KBH_4-modified electrode;
× —Simulated

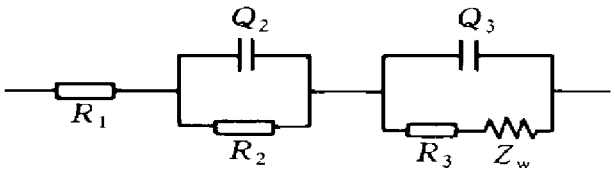

Fig. 9 Equivalent circuit for EIS of MH electrodes

R_1 —Resistance of electrolyte,
R_2 —Contact resistance between alloy particles and collector;
R_3 —Charge-transfer resistance R_{ct};
Q_i —Constant phase element,
$Q_i(\omega) = \{Y_{i0}(j\omega)^n\}^{-1}$, $0 < n \leqslant 1$;
Z_W —Warburg impedance of hydrogen diffusion,
$Z_W(\omega) = \{Y_W(j\omega)^{\alpha}\}^{-1}$, $0.5 \leqslant \alpha < 1$

As shown in Tables 1 and 2, the surface modifications considerably decrease the charge-transfer resistance and activation enthalpy of the electrode reaction on the surface. The modifications make the alloy form a Ni-rich layer with high electrocatalytic activity on surface and increase the larger specific surface area of the electrode. Hence, the activation enthalpy for dissociation of water is decreased.

Table 1 Parameters of equivalent circuit for EIS of different MH electrodes at 25 ℃ and 50% DOD

MH electrode	R_1/Ω	R_2/Ω	Y_{20}/S	n	R_3/Ω	Y_{30}/S	n	Y_w/S	α
Unmodified	0.045 9	0.018 3	0.456	0.908	0.091	1.828	0.78	899	0.68
KBH_4-modified	0.047 7	0.015 4	0.369	0.980	0.041	2.462	0.72	1 147	0.71
NaH_2PO_2-modified	0.047 3	0.016 4	0.391	0.964	0.052	2.047	0.75	963	0.69

Table 2 Effect of surface modification on activation enthalpy of MH electrode reaction

MH electrode	Unmodified	KBH_4-modified	NaH_2PO_2-modified
activation enthalpy $\Delta_r H$ / (kJ·mol^{-1})	34.2	21.6	26.6

4 CONCLUSIONS

The electrochemical performances such as activation property and discharge capacity are considerably improved by the surface modifications using KBH_4 or NaH_2PO_2 as reductants in alkaline solution. The results of CV and EIS indicate that the surface modifications apparently improve electrochemical activity on the electrodes surface and decrease the charge-transfer resistance and activation enthalpy of MH electrode reaction.

REFERENCES

1 Furukawa N. J Power Sources, 1994, 51: 45– 59.
2 Anaba A, Arnaldo V, Konstantin P *et al*. J Power Sources, 1994, 47: 261– 276.
3 Matsuoka M, Terashima M and Iwakura C. Electrochimica Acta, 1993, 38: 1087– 1092.
4 Adzic G D, Reilly J J, Makrjee S *et al*. J Electrochem Soc, 1995, 142: 3429– 3433.
5 Matsuoka M, Asai K, Fukumoto Y *et al*. J Alloys and Comp, 1993, 192: 149– 151.
6 Yan D, Sandrock G and Suda S. J Alloys and Comp, 1994, 216: 272– 242.
7 Geng M. J Alloys and Comp, 1995, 217: 90– 93.
8 Wang X L and Suda S. Z Phys Chem, 1994, 183: 385.
9 Iwakura C, Fukumoto Y, Matsuoka M *et al*. J Alloys and Comp, 1993, 192: 152– 154.
10 Wada M, Yoshinagn H and Kajita O. J Alloys and Comp, 1993, 192: 164– 160.
11 Sakai T, Miyama H, Kuriyama N *et al*. J Electrochem Soc, 1990, 137: 795– 799.
12 Kuriyama N, Sakai T and Miyamura H. J Alloys and Comp, 1993, 192: 161– 163.
13 Chen W X, Tang Z Y, Guo H T and Chen C P. J Power Sources, in press.
14 Kitamura T, Iwakura C and Tamura H. Electrochim Acta, 1982, 27: 729.

(Edited by Peng Chaoqun)